

RECORDS ADMINISTRATION



ABWS

ACC# 735328
DP-MS-82-18

**LEACHABILITY OF WASTE GLASS SYSTEMS —
PHYSICAL AND MATHEMATICAL MODELS**

by

George G. Wicks and Richard M. Wallace

E. I. du Pont de Nemours & Co.
Savannah River Laboratory
Aiken, South Carolina 29808

SRL
RECORD COPY

An invited paper for publication in
the **Journal of Nuclear Materials**

This paper was prepared in connection with work done under Contract No. DE-AC09-76SR00001 with the U.S. Department of Energy. By acceptance of this paper, the publisher and/or recipient acknowledges the U.S. Government's right to retain a nonexclusive, royalty-free license in and to any copyright covering this paper, along with the right to reproduce and to authorize others to reproduce all or part of the copyrighted paper.

This document was prepared in conjunction with work accomplished under Contract No.
DE-AC09-76SR00001 with the U.S. Department of Energy.

DISCLAIMER

This report was prepared as an account of work sponsored by an agency of the United States Government. Neither the United States Government nor any agency thereof, nor any of their employees, makes any warranty, express or implied, or assumes any legal liability or responsibility for the accuracy, completeness, or usefulness of any information, apparatus, product or process disclosed, or represents that its use would not infringe privately owned rights. Reference herein to any specific commercial product, process or service by trade name, trademark, manufacturer, or otherwise does not necessarily constitute or imply its endorsement, recommendation, or favoring by the United States Government or any agency thereof. The views and opinions of authors expressed herein do not necessarily state or reflect those of the United States Government or any agency thereof.

This report has been reproduced directly from the best available copy.

Available for sale to the public, in paper, from: U.S. Department of Commerce, National Technical Information Service, 5285 Port Royal Road, Springfield, VA 22161, phone: (800) 553-6847, fax: (703) 605-6900, email: orders@ntis.fedworld.gov online ordering: <http://www.ntis.gov/ordering.htm>

Available electronically at <http://www.doe.gov/bridge>

Available for a processing fee to U.S. Department of Energy and its contractors, in paper, from: U.S. Department of Energy, Office of Scientific and Technical Information, P.O. Box 62, Oak Ridge, TN 37831-0062, phone: (865) 576-8401, fax: (865) 576-5728, email: reports@adonis.osti.gov

**LEACHABILITY OF WASTE GLASS SYSTEMS —
PHYSICAL AND MATHEMATICAL MODELS***

by

George G. Wicks and Richard M. Wallace

E. I. du Pont de Nemours & Co.
Savannah River Laboratory
Aiken, South Carolina 29808

ABSTRACT

The corrosion of waste glass forms can be described in a 3-stage process: 1) interdiffusion, 2) matrix dissolution and 3) surface layer formation. The most important consideration in the corrosion of waste glass systems is the formation and stabilization of protective surface layers that form during leaching.

These layers are produced primarily from waste constituents that precipitate on the surface of the gel layer when the more soluble materials are leached away. The rate of subsequent leaching is believed to be controlled by the rate of dissolution of silica at the interface between the gel layer and the precipitated layer and by the rate of diffusion of dissolved silicates through the precipitated layer. A mathematical model was developed to describe leaching of these processes. This model predicts that the slope of log of the amount leached versus log time should be one initially and approach one half as the surface layer develops. The slope will further decrease if saturation in the leachant is approached.

* The information contained in this article was developed during the course of work under Contract DE-AC09-76SR00001 with the U.S. Department of Energy.

INTRODUCTION

The leachability of glass has been studied by many different techniques. Most of the theoretical work has focused on only very simple glass systems[1]. This work has lead to the identification of two main stages of glass corrosion: (1) interdiffusion and (2) matrix dissolution. These corrosion modes alone are inadequate to fully describe leaching of the more complicated waste glass systems.

Recent work at Savannah River Laboratory (SRL) has identified a further stage of corrosion for waste glass compositions, (3) surface layer formation[2]. The formation and stability of protective surface layers are believed to be the most important factors affecting long term performance of waste glass products during permanent storage.

The primary objective of this report is to analyze a growing body of leachability data to determine if existing concepts and models describing leachabilities of simple glasses apply to the more complex waste glass systems. Since the leachability behavior of waste glass forms failed to conform to existing models, a new model was developed based on diffusion of soluble components through the developing surface layers. While this model, called the SRL Leachability Model, does not yet completely describe all aspects of the leachability of SRP waste glasses quantitatively, it does represent the data more accurately than other existing models. This model will be improved as more data become available.

SUMMARY

Examination of the ratios of the concentrations of various elements in leachates and in four different glass systems revealed that the ratios were virtually independent of time within the period from three days to twenty-eight days. However, the absolute values of elemental ratios in solution differed from the corresponding ratios in the original glasses. These observations lead to the following conclusions:

- (1) The interdiffusion and matrix dissolution processes go to steady state quite rapidly at 90°C and diffusion through a surface layer is the dominant process, even in the first three days of leaching.
- (2) Glasses investigated in this study corrode congruently but only part of each component enters the solution; the remainder, primarily components from the waste, precipitate and become part of the surface layer. Different fractions of the various elements originally in the glass enter the leachate and the surface layer, hence the appearance of incongruent dissolution. The surface layer may also adsorb trace components also giving rise to the appearance of incongruent dissolution.

An SRL leachability model was developed which assumes that glass corrodes congruently and the rate of corrosion is controlled by the rate of reaction of amorphous silica with water as well as the rate of diffusion of soluble silicates through the insoluble

layer between the glass and the bulk solution. The thickness of the insoluble layer is proportional to the amount of glass that has dissolved from the start of the experiment. The silicate concentration gradient in the layer is equal to the difference between the silicate concentration at the glass layer interface and that in the bulk leachate divided by the layer thickness.

The model for waste glass corrosion assumes that Stage 1 corrosion is completed quickly. The model then predicts that the slope of log concentration vs. log time plot should be initially 1 then shift to 0.5 at a later time and finally approaches 0 as the leachate becomes saturated with silicates. The point at which the transition from a slope of 1 (matrix dissolution controlled) to 0.5 (diffusion controlled) occurs depends primarily on the ratio of the reaction rate constant to the diffusion coefficient. The point at which saturation becomes important depends primarily on the ratio of surface area of glass to volume of leachant. For large values of this ratio, saturation may become important before the shift from matrix dissolution to diffusion controlled kinetics occurs. In open systems where the products of leaching are not allowed to accumulate (but surface layers are formed) the slopes should shift from 1 to 0.5 but not drop below that value. A simple matrix dissolution model (involving no protective surface layers) predicts a slope of 1 which remains near that value until saturation becomes important when it then drops toward zero.

Experimental values of the slopes in four sets of MCC-1 tests varied between 0.5 and 0.25. The estimated fractional saturation of silicates in these tests was only sufficient to account for slopes from 0.94 to 0.76 for the matrix dissolution model and from 0.48 to 0.41 for the surface layer model. The SRL simple surface layer model is therefore superior to the matrix dissolution model in describing these experiments, but it is still not able to fully account for some of the very small slopes observed.

The pH of the leachate solutions was nearly the same after three days of leaching as after twenty-eight days. This was attributed to the buffering action of silicates and borates in solution. Values of the pH calculated from the composition of the leachates and equilibrium constants found in the literature agree reasonably well with the values measured at 25°C. Values of the pH were also calculated for the 90°C case and were used together with solubility data to estimate the degree of silica saturation at that temperature.

EVALUATION OF LEACHING RESULTS

Four different waste glasses were subjected to the MCC-1 standard leach test at 90°C in distilled water with a surface area to volume of leachant ratio of 0.1 cm⁻¹. The compositions of these glasses are shown in Table 1 and the concentration of selected elements in the leachates after 3, 7, 14, and 28 days of leaching at 90°C are shown in Tables 2 through 5. Temperature

dependence was also examined and will be discussed in a later report. These tables contain the raw data upon which subsequent arguments will be based.

pH of Leachates

One of the most striking features about these leaching data is that the pH of the leachates stabilized within the first three days and changed very little thereafter. If interdiffusion were the predominant process, we would expect the pH to increase in the early stages due to the increased concentration of alkali hydroxides in the leachate. This process was completed within the first three days and the interdiffusion and matrix corrosion processes have gone to steady state within that period.

The pH does not reach higher values because of the buffering action of silicate and borate in the leachate. To demonstrate this point, the pH of each of the solutions at 25°C was calculated from the composition of the solutions using methods described in the Appendix and values of the equilibrium constants found in the literature. These pH values, shown in Table 6, agree fairly well with the experimental values also shown.

The values of pH in solution were not measured at 90°C, the temperature of the leaching experiments. To evaluate the leaching models it was necessary to know the degree of saturation of silica in solution at the pH and temperature of the experiments. The values of pH at 90°C for the leachate solutions were calculated

from values of the equilibrium constants found in the literature. The silicate solubilities were then calculated from these values of the pH and literature values of the solubility of amorphous silica in water, using the methods described in the Appendix. These values are also shown in Table 6.

Ratios of Elements in Leachates

Further insight into leaching mechanisms was obtained by taking the ratios of the concentrations of the various components in the leachates. These are shown in Table 7 together with the corresponding ratios in the original glasses. It was surprising that these ratios were virtually constant. If an interdiffusion and matrix dissolution process were in operation one would expect an initially high ratio of network modifiers (Na, K, Li) to network formers (Si) followed by a gradual decrease in the ratio as steady state is approached. There appears to be a slight trend of this sort with the NBS glass but one in the reverse direction with 76-68 glass. In neither case is the variation greater than 20%.

The variations of the ratios with time are not nearly as large as the difference between the ratios in solution and those in the original glass, as can be seen in Table 8. Here the average over time of each ratio is given together with the corresponding ratios in the original glass and the quotient of the ratio in solution divided by the ratio in the glass. A value of this quotient greater than one implies a relative enrichment in

solution of the component in the numerator over that in the denominator; a value less than one implies relative depletion. Thus, in all solutions, boron and the alkali elements (Li, Na, K) are enriched relative to silicon. With the glasses containing waste (76-68, SRL-1 and SRL-2), the alkali elements are slightly enriched in the leachate relative to boron, while in the NBS glass potassium was depleted relative to boron; aluminum was also depleted relative to boron in the two cases examined. Other elements such as iron and strontium were also probably depleted relative to boron and the alkali elements in the waste glasses because only very small quantities of these elements were found in the leachate. These elements, however, were not studied in detail. The quotients were nearly the same from one glass to the next among those containing waste but some of the quotients for NBS glass were significantly different from the others.

The preceding observations are consistent with the following picture of the glass corrosion process. The process of inter-diffusion and matrix dissolution have come to steady state at 90°C long before the end of the first three-day leaching period and the predominant mode of leaching involves congruent corrosion of the glass followed by diffusion of soluble components through the surface layer. As the glass reacts with water, a certain fraction of each element will enter solution and another fraction will react with other components in the system to precipitate and form an addition to the surface layer. Thus, some silica will enter

solution as sodium silicate while another fraction will precipitate as calcium silicate or form an alumino silicate gel. Since alkali ions and borates are less likely to form insoluble compounds than silicon, these elements will tend to be enriched relative to silicon in the leachate. This picture of the leaching process accounts for constant ratios of elements in the leachates that are markedly different from those in the original glass.

SURFACE LAYER FORMATION

The above view has been strengthened by the discovery and subsequent characterization of protective surface layers that form on glass during the leaching process, particularly in waste glasses. The importance of waste constituents on surface layer formation, stability, and chemical durability of the product has been investigated and reported elsewhere[2,3].

Analytical techniques for studying leached glass surfaces have been pioneered by L. L. Hench and coworkers at the University of Florida[1]. These techniques have been further developed at Savannah River and are summarized schematically in Figure 1.

The surface layers that form over the glass during leaching are shown in Figure 2. These layers adhere relatively tightly to the glass underneath and are usually at least several microns thick. X-ray line profiles from SEMQ (electron microprobe) micrographs are shown for four key elements in Figure 3. More quantitative analysis of elements of interest in precipitated surface

layers and bulk glass are given in Tables 9 and 10 with an accompanying Auger depth profile in Figure 4. The surface layers are relatively enriched in major elements of the waste including iron and manganese and relatively depleted in major constituents of the glass frit, including silicon and sodium, compared to the bulk waste glass. These compositional analyses provide insight into the importance of waste constituents in formation and stabilization of surface layers. Accompanying leachability data show that these layers result in leachability decreasing with time.

The importance of the nonradioactive species of the waste on surface layer formation is further demonstrated in a recent study which evaluated leachability as a function of waste loading (Table 11). The composition of the surface layers for glasses containing waste were very different than for pure frit with no waste. Leached glasses containing no waste produced silica enriched surface layers while leached waste glass contained surface layers depleted in silica. Figure 5 shows the leachability of SRP waste glass as a function of waste loadings ranging from 0 to 50 wt % oxides. As observed in this graph, the leachability of the product actually improves with increased waste loading. This is a direct result of protective surface layers that form from elements of the waste. From the micrographs in Figures 6 and 7, we note that there is a direct correlation with surface layer thickness and product leachability. The thinner, and perhaps more dense, adherent layers protected the glass underneath more effectively than the thicker and more friable surface layers[3].

PHYSICAL MODEL AND STAGES OF CORROSION OF WASTE GLASS FORMS

There are three basic roles that elements of the waste or frit can play in the random network structure of the glass. These roles depend on such considerations as the cation-oxygen bond strengths.

The most important roles of cations in waste glass systems are as "network formers." This is exemplified by elements of the frit such as Si and B which form the backbone structure of the glass about which oxygen polyhedra are coordinated. Cations can also act as "intermediates" and either join into the framework or occupy holes within the network structure and are exemplified by elements such as Al. The third and perhaps dominant role of cations are as "modifiers" and include alkali and alkali-earth species of both frit and waste. The modifier cations fit into holes within the network structure and associate with nonlinking or newly created singly bonded oxygens. Therefore, elements of both the frit as well as waste can be bound into the structure by different means and to a variety of degrees, resulting from various primary and/or secondary bonding forces. Hence, based on the basic structure of glass alone one would not expect the leachability of all elements to necessarily be the same. It is therefore necessary to consider many different elements and their individual "leachabilities" to understand fully the mechanisms of glass corrosion.

A physical interpretation of the corrosion processes involved for the SRP waste glass forms can be described in terms of a structural 3-stage corrosion process. This represents an extension of the 2-stage corrosion process proposed by Hench for simpler glass systems[1]. These stages become the building blocks of the more quantitative model that will follow and are illustrated schematically in Figure 8.

3-Stage Corrosion Process of SRP Waste Glass

● Stage 1 — Interdiffusion

Interdiffusional processes dominate the early stages of glass corrosion. Network modifiers such as sodium and potassium, diffuse out of the glass into solution during leaching while water from the leachant diffuses into the glass at the same time. This results in a modifier deficient or silica enriched surface layer. Mathematical analysis of this process leads to the conclusion that the concentration of diffusing species in the leachate should increase as the square root of the time, a conclusion verified experimentally for simple glass[1,4]. During this time period, the pH of the leachant increases due to formation of alkali hydroxides in solution.

● Stage 2 — Matrix Dissolution

This process is expected to dominate at intermediate leaching times. The dissolution rate is governed by the pH of the leachate which determines the solubility of amorphous silica. The glass

dissolution rate may be controlled simply by the rate at which the silica in a saturated solution near the surface can diffuse away from the glass into the bulk solution; it is possible, however, that hydroxide ions might directly affect the rate of reaction between silica and water. If the composition of the solution were to remain constant, the rate of dissolution of the matrix would also be expected to remain constant, and the concentration of network formers in solution, such as silicon, would increase linearly with the first power of the time. This dependence has been observed in simple glass systems. In a closed system where the products of leaching are allowed to accumulate, the dissolution rate is expected to increase as the pH increases, but slow down later as the solution becomes saturated with silicates. After a sufficiently long time, the rate of the diffusional processes should be equal to the rate of dissolution (steady state) and congruent dissolution should result if only the two processes are involved.

● Stage 3 — Surface Layer Formation

During intermediate and long time periods, surface layers can form on waste glass forms[2] resulting from the precipitation of insoluble compounds on the glass surface. These layers may contain compounds such as ferric hydroxide, manganese dioxide or calcium silicate. The existence of similar layers on the surface of even simple glasses has been conjectured[1] to affect the

leachability of glass but no detailed formulation of how these layers should affect the leach rate has yet been made.

MATHEMATICAL MODEL

Figure 9 shows the developing precipitated surface layer of thickness ℓ between the hydrated silica gel layer of the glass and the bulk leachate. C_0 is the concentration of silicate at the glass layer interface while C is the silicate concentration in the leachate. The model was developed using the following assumptions.

Assumptions

- (1) Steady state has been attained with respect to the first two processes so that glass corrodes congruently at the beginning of this process.
- (2) The surface of the glass initially consists principally of amorphous silica as will the interface between the glass and the developing surface layer of insoluble material.
- (3) The rate of dissolution of amorphous silica at that interface will be given by

$$\Theta = K (C_s - C_0) \quad (1)$$

Where Θ is the number of millimoles of silica dissolved per unit time per cm^2 . K is the rate constant, C_s is the concentrate of saturated silica and C_0 is the silicate concentration at the interface within the layer.

- (4) The rate will also be controlled by the rate at which silicate can diffuse through the layer of insoluble material.
- Thus, if steady state is assumed within the layer

$$\Theta = \frac{D}{l} (C_o - C) \quad (2)$$

where D is the diffusion coefficient of silicate within the layer, l is the layer thickness, and C is the silicate concentration in solution.

- (5) The amount of material in the surface layer and hence its thickness will depend on the amount of glass that has corroded since the beginning of the experiment, and therefore on the total amount of silicate, L, leached up to time t.

Therefore:

$$l = qL \quad q \text{ is a constant} \quad (3)$$

The total rate of silica dissolved as expressed in Equations

- (1) and (2) can be written in a more convenient form

$$\Theta = K_r (1 - y_o) \quad (4)$$

$$\Theta = K_d (y_o - y) \quad (5)$$

where $y \equiv C/C_s$; $y_o \equiv C_o/C_s$

$$K_r \equiv KC_s; K_d \equiv \frac{DC_s}{l} \quad (6)$$

Combining (4) and (5) we get

$$y_o = \frac{K_r + K_d y}{K_r + K_d}$$

$$\text{and } \Theta = \frac{K_r K_d (1 - y)}{K_r + K_d} \quad (8)$$

The rate of silica dissolution by definition is

$$\Theta = \frac{dL}{dt} \quad (9)$$

Combining Equations (3), (7), and (8) and the definitions in (6), we obtain

$$\frac{dL}{dt} = \frac{K_r (1 - y)}{1 + \beta L} \quad (10)$$

$$\text{where } \beta \equiv \frac{Kq}{D}$$

Equation (10) applies in general to silica dissolution from the waste glass while y , the fractional saturation of the leaching solution, may or may not be a function of the time or the amount of glass leached.

In the special case of a closed system, where the products of leaching are allowed to accumulate in the leachant, y will be a function of L and can be written as

$$y = \alpha L \quad (11)$$

$$\text{where } \alpha \equiv \frac{A}{VC_s} \quad \begin{array}{l} A = \text{surface area of glass} \\ V = \text{volume of leach solution} \end{array}$$

Equation (11) then becomes

$$\frac{dL}{dt} = \frac{K_r (1 - \alpha L)}{1 + \beta L} \quad (12)$$

Integration of (12) subject to the initial conditions that

$L = 0$ when $t = 0$ yields

$$(1 + \beta/\alpha) \ln (1 - \alpha L) + \beta L = \alpha k_r t \quad (13)$$

and in the limiting case where $\alpha = 0$

$$L + \frac{\beta L^2}{2} = K_r t \quad (14)$$

The properties of these functions are more conveniently examined if they are written in terms of dimensionless variables

$$X \equiv \beta L; \gamma \equiv \alpha/\beta; \tau \equiv \beta K_T t.$$

Equations (13) and (14) then become

$$\frac{1}{\gamma} [(1 + 1/\gamma) \ln (1 - \gamma x) + x] = \tau \quad (13')$$

$$x + \frac{x^2}{2} = \tau \quad (14')$$

It is frequently useful to determine the slope of a log L vs. log t to determine if the theoretical slopes agree with those obtained experimentally. These slopes can be obtained from Equations (13) and (14) since

$$\frac{d \log L}{d \log t} = \frac{t}{L} \frac{dL}{dt}$$

when written in terms of dimensionless variables, these slopes are:

$$\text{slope} = - \frac{1}{\gamma x} \frac{(1 - \gamma x)}{(1 + x)} [(1 + 1/\gamma) \ln (1 - \gamma x) + x] \quad (15)$$

In the limit as $\gamma \rightarrow 0$,

$$\text{slope} = \frac{1 + x/2}{1 + x} \quad (16)$$

Figure 10 shows the slopes of the log L vs. log t plots, derived from Equations (15) and (16), as a function of $\log_{10} x$ for various values of the parameter γ . $\log_{10} x$ was used as the abscissa simply to expand the scale. When $\gamma = 0$ (i.e., $A/V = 0$) the slopes start at one for small values of x, shift toward lower values near $x = 1$ ($\log_{10} x = 0$) and finally level off at 0.5 for large

values of x . The portion of the curve where the slope is one represents a condition where the precipitated layer is so thin (or is very porous with a large D) that the leach rate is controlled entirely by matrix dissolution. In the region near $x = 1$ bulk matrix dissolution and diffusion are involved in controlling the leach rate while at large values of x (thick layers) it is controlled almost entirely by layer diffusion.

When γ is small but finite, the slope again starts at one for small values of x , shifts to lower values near $x = 1$, levels off to values near 0.5 for large values of x but then drops below 0.5 and approaches 0 as saturation is approached (i.e., $x = 1/\gamma$). For large values of γ , the transition of the slope from one to zero occurs before the transition from one to 0.5 near $x = 1$. This represents a condition in which the surface area to volume ratio is so large that saturation occurs before the layer has grown thick enough to affect the leach rate.

In the limit as γ becomes very large Equations (13') and (15) respectively approach:

$$\ln(1 - y) = -\alpha K_r t; \text{ slope} = -\frac{(1 - y)}{y} \ln(1 - y)$$

and for small values of γ they approach

$$\ln(1 - y) + y = -\frac{\alpha^2}{\beta} K_r t; \text{ slope} = -\frac{(1 - y)}{y^2} (\ln(1 - y) + y)$$

The first set of equations are those we would derive for a simple matrix dissolution model while the second are those we can derive for a model in which the only process is diffusion through

the layer from a silica saturated solution near the glass-layer interface.

These equations are convenient to compare with experiment because the empirically determined slopes at various values of the fractional saturation (y) can be compared with those predicted theoretically.

Values of the slopes for both models as a function of y are given in Table 12.

Comparison of Experimental Slopes of Log-Log Plots with Theory

Table 13 contains the slopes, S , of the lines obtained when a function of the form

$$\log (C_i) = A + S \log (t)$$

was fit by least squares to the experimental leaching data in Tables 2-5. Here C_i is the concentration of the i 'th component in solution, t is the time in days from the beginning of the experiment and A is a constant. Also shown are the correlation coefficients, R , which show how well the data were fit by the equation.

All of the slopes are less than 0.5 and far less than the value of 1.0 one would expect for a simple matrix dissolution model. To see how well these slopes correspond to those predicted by the layer and the matrix dissolution model, the average values of the slopes for those elements for which the correlation coefficient were 0.95 or greater was taken for each glass. These are

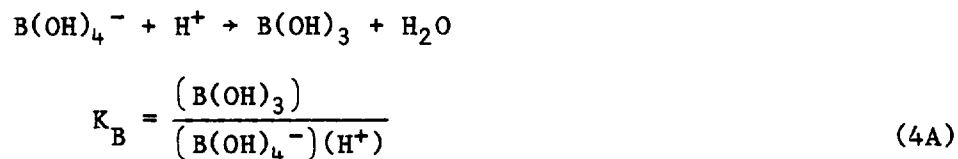
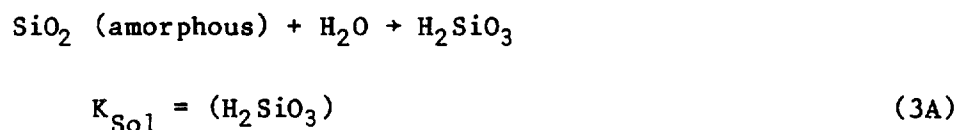
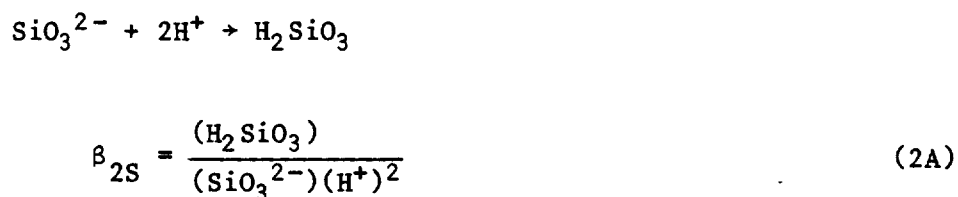
shown in Table 14 together with the maximum degree of saturation calculated for each of the glasses as described in the pH section. The average slopes are to be compared with those predicted by the two models at that value of the saturation.

Table 14 shows that the surface layer model gives a better representation of the data than the matrix dissolution model, a model that severely overpredicts dissolution of waste glass systems. However, the agreement with experiment is far from perfect. It is possible that the equilibrium constants used for the calculation of silica saturation at 90°C are in error. It is more likely that the simple surface layer model needs refinement before it can adequately describe quantitative leaching behavior.

APPENDIX

CALCULATION OF LEACHATE pH VALUES AND SILICA SOLUBILITY OF SRP WASTE GLASS FORMS

The following equilibria were considered in estimating the pH and equilibrium solubility of silica in leachate solutions from their chemical composition:



Mass balance on silicate species yields

$$(\text{Si}_t) = (\text{SiO}_3^{2-}) + (\text{HSiO}_3^-) + (\text{H}_2\text{SiO}_3) \quad (6A)$$

where (Si_t) is the total silicate concentration in solution.

Combining Equations (1A) and (2A) with (3A)

$$(\text{Si}_t) = (\text{SiO}_3^{2-})[1 + K_{1S}(\text{H}^+) + \beta_{2S}(\text{H})^2] \quad (7A)$$

$$\text{Let } Q_S \equiv [1 + K_{1S}(\text{H}) + \beta_{2S}(\text{H})^2]$$

$$\text{then } (\text{SiO}_3^{2-}) = \frac{(\text{Si}_t)}{Q_S} \quad (8A)$$

$$(\text{HSiO}_3^-) = \frac{K_{1S}(\text{H})(\text{Si}_t)}{Q_S} \quad (9A)$$

$$(\text{H}_2\text{SiO}_3) = \frac{\beta_{2S}(\text{H})^2(\text{Si}_t)}{Q_S} \quad (10A)$$

Mass balance on boron species

$$(\text{B}_t) = (\text{B(OH)}_3) + (\text{B(OH)}_4^-) \quad (11A)$$

$$(\text{B}_t) = (\text{B(OH)}_4^-)[1 + K_B(\text{H})] \quad (12A)$$

$$\text{Let } Q_B \equiv [1 + K_B(\text{H})]$$

$$\text{then } (\text{B(OH)}_4^-) = \frac{(\text{B}_t)}{Q_B} \quad (13A)$$

$$(\text{B(OH)}_3) = \frac{K_B(\text{H})(\text{B}_t)}{Q_B} \quad (14A)$$

Charge balance in solution yields

$$(\text{H}^+) + \sum_i C_i Z_i = (\text{B(OH)}_4^-) + 2(\text{SiO}_3^{2-}) + (\text{HSiO}_3^-) + (\text{OH}^-) \quad (15A)$$

where C_i is the concentration of the i 'th cation in solution and Z_i is its charge combining Equations (5A), (8A), (9A), (13A) and (15A)

$$-(H) + \sum_i \bar{Z}_i C_i Z_i = \frac{(B_t)}{Q_B} + \frac{(S_{it})}{Q_S} (2 + K_{1S}(H)) + \frac{K_W}{(H)} = 0 \quad (16A)$$

the equilibrium pH of the solution will be found by solving Equation (16A) for (H) . Since it is a fifth order Equation in (H) it is most easily solved numerically.

We know at the outset the solution lies somewhere between pH 0 and pH 14. We can then set these values as limits, take the average and substitute the corresponding value (H) into (16A). If the result is a positive number, the average pH was too high, and may be substituted as a new upper limit; if the result is negative, the pH chosen was too low and may be substituted as a new lower limit. The procedure is then repeated successively until the desired accuracy is obtained. Twelve iterations are sufficient to reduce the error to less than 0.01 pH units.

When the pH is known the equilibrium solubility of silica may be determined by combining Equations (3A) and (10A).

$$(S_{it}) = \frac{K_{Sol} Q_S}{\beta_{2S} (H)^2} \quad (17A)$$

Equation (17A) is the basis for theoretically predicting silica saturation as a function of solution pH. The calculated values at 90°C are shown in Table 6. These data become important in determining the degree of saturation of silica in solution during leaching.

The following constants were used to make the numerical calculations:

<u>T</u>	<u>Log K_{1S}</u>	<u>Log β_{2S}</u>	<u>Log K_B</u>	<u>Log K_W</u>	<u>K_{sol}</u>
25°C	11.77	21.28	9.24	-14.00	0.0012M
90°C	9.90	18.98	8.62	-12.42	0.0065M
Reference	[5]	[5]	[6]	[7]	[8]

REFERENCES

- [1] D. E. Clark, C. G. Pantano and L. L. Hench, Corrosion of Glass, Books for the Glass Industry (1979).
- [2] G. G. Wicks, W. C. Mosley, P. G. Whitkop and K. A. Saturday, Durability of Simulated Waste Glass — Effects of Pressure and Formation of Surface Layers, DP-MS-81-25, presented at the 6th University Series on Glass Science, University Park, Pennsylvania, July 29-31, 1981. To be published in Journal of Non-Crystalline Solids.
- [3] W. D. Rankin and G. G. Wicks, The Chemical Durability of Savannah River Plant Waste as a Function of Waste Loading, to be presented at the 84th Annual Meeting and Exposition of the American Ceramic Society, Cincinnati, Ohio, May 2-5, 1982 and proposed for publication in Journal of American Ceramic Society.
- [4] R. W. Douglas and T. M. El-Shamy, Reactions of Glasses with Aqueous Solutions, J. Amer. Cer. Soc., 50(1) pp. 1-8 (1967).
- [5] Stability Constants, p. 145, Chemical Society, London, 1964, Special Publication No. 17.
- [6] Ibid, p. 105.
- [7] H. S. Harned and B. B. Owen, The Physical Chemistry of Electrolytic Solutions, p. 645, Reinhold, New York, 1958.
- [8] W. F. Linke and A. Seidell, Eds., Solubility of Inorganic and Metal Organic Compounds, fourth ed. Vol. II, p. 1452, American Chemical Society, Washington, 1965.

Table 1
Glass and Waste Glass Compositions Used in MCC-1 Static Leach Tests

Compound	Glass System			
	NBS ^{a)}	76-68 ^{b)}	SRL-1 ^{c)}	SRL-2 ^{d)}
Rb ₂ O		0.13		
SrO		.40	.02	0.1
Y ₂ O ₃		.23		
ZrO ₂		1.88	ND	ND
MoO ₃		2.42		
CdO		.04		
Cs ₂ O		1.09	.04	0.3
BaO		0.49		
La ₂ O ₃		.56		
CeO ₂		1.26		0.1
Pr ₆ O ₁₁		.56		
Nd ₂ O ₃		4.56	ND	0.7
Sm ₂ O ₃		0.35		
Eu ₂ O ₃		.10		
Gd ₂ O ₃		.05		
Fe ₂ O ₃		10.34	12.6	13.8
Cr ₂ O ₃		0.44		
NiO		.21	1.43	
P ₂ O ₅		.51		
CaO		2.00	1.06	
ZnO		4.97		
TiO ₂		2.97	ND	ND
Na ₂ O	1.0	12.80	12.3	13.5
SiO ₂	70.0	39.80	52.8	44.8
B ₂ O ₃	17.0	9.47	10.4	9.9
K ₂ O	8.0			
Li ₂ O ₃	1.0		3.79	ND
Al ₂ O ₃	3.0		5.91	2.6
MnO ₂			3.29	4.3
MgO			0.38	ND
La ₂ O ₃			0.4	ND
U ₃ O ₈				0.6

a) NBS glass contains no waste — analyses supplied by vendor.

b) 76-68 is commercial waste glass — analyses from batch makeup by PNL.

c) SRL-1 is an experimental S.R. defense waste glass — analyses of solidified product by AA and IC.

d) SRL-2 is an actinide doped S.R. defense waste glass — analyses of solidified product by ICP, AA and IC.

Table 2

Concentration of Selected Elements in Leachate at 90°C
(MCC-1 Standard Leach Tests)

Leach Time		NBS Glass (No Waste)					
Days		Si	B	Na	K	Al	pH
3	mg/l	44.6	16.7	2.66	15.3	1.29	8.50
	M	1.59E-3	1.54E-3	1.66E-4	3.90E-4	4.77E-5	
7	mg/l	48.5	17.1	2.16	16.2	2.21	8.45
	M	1.73E-3	1.58E-3	9.39E-5	4.14E-4	8.19E-5	
14	mg/l	73.0	24.7	2.12	21.9	2.02	8.46
	M	2.60E-3	2.29E-3	9.21E-5	5.60E-4	7.48E-5	
28	mg/l	80.9	28.2	3.28	24.1	1.85	8.64
	M	2.80E-3	2.61E-3	1.42E-4	6.17E-4	6.85E-5	

Table 3
Concentration of Selected Elements in Leachate at 90°C
(MCC-1 Standard Leach Tests)

Leach Time		76-68 Waste Glass				
Days		Si	B	Na	Cs	pH
3	mg/l	24.6	4.90	17.3	.33	9.23
	M	8.76E-4	4.53E-4	7.52E-4		
7	mg/l	36.8	7.53	28.1	.24	9.29
	M	1.31E-3	6.96E-4	1.22E-3		
14	mg/l	46.5	10.3	36.8	.43	9.39
	M	1.65E-3	9.53E-4	1.60E-3		
28	mg/l	61.5	14.3	53.9	.63	9.56
	M	2.19E-3	1.32E-3	2.34E-3		

Table 4
Concentration of Selected Elements in Leachate at 90°C
(MCC-1 Standard Leach Tests)

Leach Time		SRL-1 Waste Glass					
Days		Si	B	Na	Li	Al	pH
3	mg/l	21.7	4.12	13.1	2.52	2.32	9.38
	M	7.73E-4	3.81E-4	4.69E-4	3.63E-4	8.59E-5	
7	mg/l	29.3	5.65	16.9	3.27	2.89	9.49
	M	1.04E-3	5.23E-4	7.34E-4	4.71E-4	1.07E-4	
14	mg/l	36.8	7.23	21.9	4.35	3.09	9.54
	M	1.31E-3	6.69E-4	9.53E-4	6.27E-4	1.44E-4	
28	mg/l	40.2	7.70	24.5	(4.85)*	4.52	9.61
	M	1.43E-3	7.12E-4	1.06E-3	(6.99E-4)*	1.67E-4	

* Estimated

Table 5
Concentration of Selected Elements in Leachate at 90°C
(MCC-1 Standard Leach Tests)

Leach Time		SRL-2 Waste Glass				pH
Days		Si	B	Na	Cs	
3	mg/l	26.6	5.18	22.8	.54	10.52
	M	9.48E-4	4.79E-4	9.90E-4		
7	mg/l	31.4	6.26	22.6	.59	9.87
	M	1.12E-3	5.79E-3	9.84E-4		
14	mg/l	45.4	9.46	36.7	.55	10.01
	M	1.62E-3	8.75E-4	1.59E-3		
28	mg/l	56.3	12.4	38.3	.59	10.10
	M	2.00E-3	1.15E-3	1.66E-3		

Table 6
pH and Solubility in Leachate Solutions

Time Days	pH 25°C ^{a)} obs	pH 25°C calc	pH 90°C calc	(Cs) 90°C ^{b)} calc M	(y=C/Cs) 90°C ^{c)}
NBS Glass					
3	8.50	8.63	8.09	.0072	.22
7	8.45	8.61	8.07	.0071	.24
14	8.46	8.55	8.01	.0071	.37
28	8.64	8.57	8.01	.0071	.41
76-68 Waste Glass					
3	9.23	9.48	8.72	.0095	.092
7	9.29	9.57	8.82	.0103	.13
14	9.39	9.58	8.86	.0108	.15
28	9.56	9.68	8.85	.0107	.20
SRL-1 Waste Glass					
3	9.36	9.89	8.91	.0113	.068
7	9.49	9.84	8.94	.0117	.089
14	9.54	9.90	9.00	.0126	.10
28	9.61	9.95	9.04	.0132	.11
SRL-2 Waste Glass					
3	10.52	9.70	8.85	.0106	.089
7	9.87	9.51	8.77	.0099	.113
14	10.01	9.62	8.88	.0110	.147
28	10.10	9.43	8.77	.0099	.20

- a) All pH measurements of leachates taken after solutions cooled from 90°C to 25°C.
b) (Cs)(90°C) denotes saturation of amorphous silica in solution of given pH.
c) Denotes ratio of silicon in leachate to saturated silica solution for given pH.

Table 7
Observed Elemental Atomic Ratios in Leachates and Original Glasses

Leach Time Days	(Na,K)/B	(Na,K)/Si	B/Si	Al/B	Na/Li
<u>NBS Glass</u>					
Original Glass	.348 (K)	.146 (K)	.419	1.20	
3	.253	.245	.969	.0310	
7	.262	.241	.919	.0518	
14	.245	.210	.881	.0327	
28	.236	.214	.906	.0262	
<u>76-68 Waste Glass</u>					
Original Glass	1.52 (Na)	.624 (Na)	.411		
3	1.66	.858	.517		
7	1.75	.931	.531		
14	1.67	.970	.578		
28	1.77	1.068	.603		
<u>SRL-1 Waste Glass</u>					
Original Glass	1.33 (Na)	.452 (Na)	.340	.388	1.56
3	1.49	.736	.492	.225	1.57
7	1.40	.706	.503	.205	1.55
14	1.42	.727	.511	.215	1.52
28	1.49	.741	.499	.235	--
<u>SRL-2 Waste Glass</u>					
Original Glass	1.53 (Na)	.583 (Na)	.381		
3	2.06	1.04	.505		
7	1.70	0.88	.517		
14	1.82	0.98	.540		
28	1.44	0.83	.575		

Table 8
Summary of Elemental Ratios

	NBS Glass	76-68 Waste Glass	SRL-1 Waste Glass	SRL-2 Waste Glass
[(K,Na)/B] L	.249 ±.011 (K)	1.71 ±.056 (Na)	1.45 ±.047 (Na)	1.76 ±.26 (Na)
[(K,Na)/B] G	.348	1.52	1.33	1.53
L/G	.714	1.13	1.09	1.15
[(K,Na)/Si] L	.228 ±.018 (K)	.957 ±.087 (Na)	.728 ±.015 (Na)	.933 ±.095 (Na)
[(K,Na)/Si] G	.146	.624	.452	.583
L/G	1.56	1.53	1.61	1.60
[B/Si] L	.919 ±.037	.557 ±.040	.502 ±.007	.545 ±.024
[B/Si] G	.419	.411	.340	.381
L/G	2.19	1.35	1.48	1.43
[Na/Li] L			1.55 ±.02	
[Na/Li] G			1.56	
L/G			1.00	
[Al/B] L	.0354 ±.011		.220 ±.013	
[Al/B] G	.120		.388	
L/G	.295		.763	

L = Leachate
G = Glass

Table 9
 SEMQ Analyses* of TDS-131 Leached in Distilled Water
 for 30 Days at 90°C

Element	Leached at 14.7 psi			Leached at 1500 psi	
	Bulk Glass	Surface Layer	"Subsurface"**	Surface Layer	"Subsurface"
Ca	0.4*	1.1	0.6	1.0	0.5
Cs	0.0	0.0	0.0	0.0	0.0
Ti	0.4	1.0	0.5	0.9	0.4
La	0.3	0.6	0.4	0.6	0.4
Ce	0.1	0.1	0.1	0.1	0.1
Nd	0.1	0.1	0.1	0.2	0.1
Mn	2.2	7.0	2.3	5.4	2.4
Fe	8.9	15.6	9.6	20.9	9.6
Ni	0.3	1.2	0.3	0.9	0.3
Zn	0.0	0.0	0.0	0.0	0.0
P	0.1	0.1	0.0	0.0	0.0
Zr	0.3	0.4	0.3	0.5	0.4
S	0.1	0.0	0.1	0.1	0.2
Cl	0.0	0.0	0.0	0.0	0.0
F	0.0	0.0	0.0	0.0	0.0
Na	12.8	0.8	10.8	1.9	11.5
Mg	0.9	3.1	0.8	2.1	0.9
Al	2.3	3.0	2.3	2.4	2.1
Si	15.9	9.6	16.4	10.1	16.4
Sr	0.0	0.0	0.0	0.0	0.0
U	0.0	0.0	0.0	0.0	0.0
K	0.0	0.0	0.0	0.0	0.0

* Composition in wt %.

** "Subsurface" layer denotes region directly below surface layer.
 The composition of this area is similar to the bulk glass.

Table 10

Auger Analyses of TDS/131 Leached in Distilled Water
for 30 Days at 90°C

Element	Leached at 14.7 psi		Leached at 1500 psi
	Bulk Glass	Outermost Surface Layer, 15A	Outermost Surface Layer, 15A
Fe	2.3*	6.1	3.2
Ni	0.4	0.8	2.5
Mg	0.7	5.0	10.7
Al	3.1	12.9	0.5
Si	59.9	40.7	37.8
Na	1.1	Trace	Trace
Mn	Trace**	Trace	1.1
B	Trace	Trace	Trace
Ca	Trace	Trace	Trace

* Composition in relative atom percent. Peak heights measured with three percent standard deviation.

** Trace denotes less than 0.1 atom percent.

TABLE 11
Waste Glass Compositions (TDS/131)

	TDS Waste (wt %) in Glass Made with Frit 131							
	0	10	20	25	30	35	40	50
SiO ₂	57.9	52.5	47.1	44.5	41.8	39.1	36.4	31.0
Na ₂ O	17.7	16.2	14.8	14.1	13.3	12.6	11.9	10.4
B ₂ O ₃	14.7	13.2	11.8	11.0	10.3	9.6	8.8	7.4
TiO ₂	1.0	0.9	0.8	0.8	0.7	0.7	0.6	0.5
Li ₂ O	5.7	5.1	4.6	4.3	4.0	3.7	3.4	2.9
MgO	2.0	1.8	1.6	1.5	1.4	1.3	1.2	1.0
ZrO ₂	0.5	0.5	0.4	0.4	0.4	0.3	0.3	0.3
La ₂ O ₃	0.5	0.5	0.4	0.4	0.4	0.3	0.3	0.3
Fe ₂ O ₃		4.7	9.4	11.7	14.0	16.4	18.7	23.4
MnO ₂		1.3	2.7	3.4	4.0	4.7	5.4	6.7
Zeolite		1.0	2.0	2.5	3.0	3.5	4.0	5.1
Al ₂ O ₃		0.9	1.9	2.4	2.8	3.3	3.8	4.7
NiO		0.6	1.1	1.4	1.7	2.0	2.3	2.9
CaO		0.4	0.7	0.9	1.1	1.2	1.4	1.8
Coal		0.2	0.5	0.6	0.7	0.8	0.9	1.2
Na ₂ SO ₄		0.1	0.1	0.2	0.2	0.2	0.2	0.3
Cs ₂ CO ₃		0.1	0.1	0.1	0.2	0.2	0.2	0.3
SrCO ₃		0.1	0.1	0.1	0.2	0.2	0.2	0.3

Table 12
Slopes of Log y vs. Log t Plot as a Function of y

y*	dlny/dlnt**	
	Surface Layer	Matrix Dissolution
0	0.50	1.0
0.1	0.48	.94
0.2	0.46	.89
0.3	0.44	.83
0.4	0.42	.77
0.5	0.39	.69
0.6	0.35	.61
0.7	0.31	.51
0.8	0.25	.40
0.9	0.17	.26
1.0	0.00	0.00

* y represents the degree of silica saturation in solution (S_i/S_{i0}).

** $\frac{d\ln y}{d\ln t}$ represents a reaction rate parameter for a Stage 3 corrosion process (Surface Layer Formation) and for a Stage 2 process (Matrix Dissolution).

Table 13
Slopes of Log Concentration vs. Log Time Plots

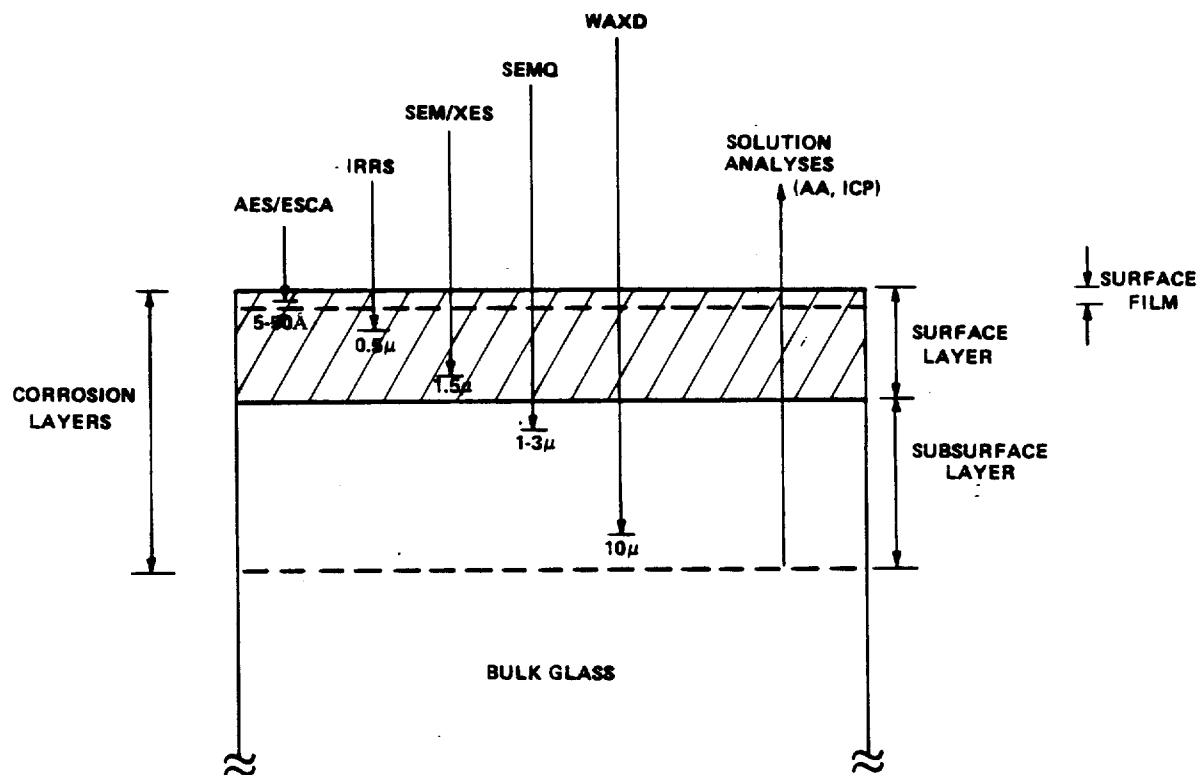
	Si	B	Na	K or Li	Al	Cs
<u>NBS Glass</u>						
S	0.294	0.258	0.074	0.223 (K)	0.144	--
R	0.953	0.939	0.345	0.955	0.585	--
<u>76-68 Waste Glass</u>						
S	0.405	0.477	0.499			0.327
R	0.997	0.999	0.997			0.765
<u>SRL-1 Waste Glass</u>						
S	0.283	0.290	0.290	0.305 (Li)	0.278	
R	0.983	0.975	0.991	0.989	0.958	
<u>SRL-2 Waste Glass</u>						
S	0.351	0.407	0.272			0.027
R	0.984	0.985	0.896			0.565

S = Slope

R = Correlation coefficient

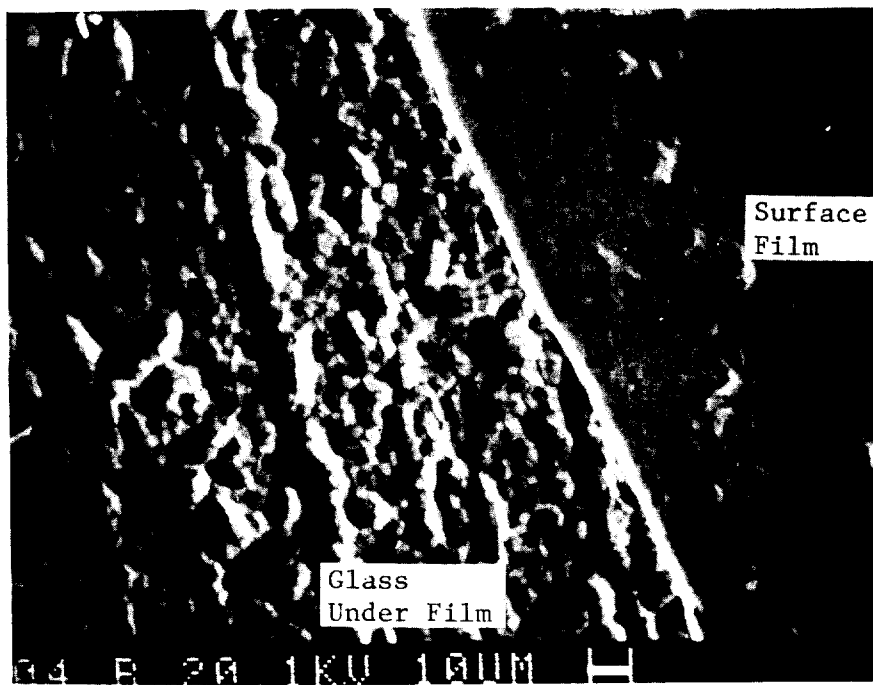
Table 14
Comparison of Experimental Slopes with Those Predicted by Models

Glass	$y = \text{Si/Si}_0$	Slope Observed	Calculated Slope	
			Layer Model	Matrix Dissolution
NBS Glass	.41	.26	.41	.76
76-68 Waste Glass	.20	.46	.46	.89
SRL-1 Waste Glass	.11	.29	.48	.94
SRL-2 Waste Glass	.20	.38	.46	.89

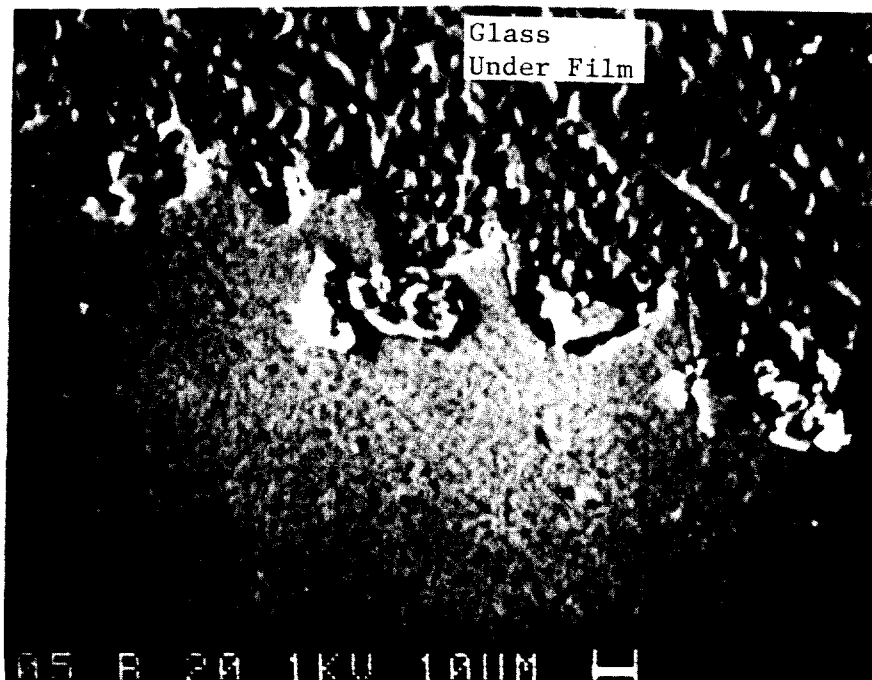


*Beam penetration generally increases with voltage (kV) and decreases with increasing sample density (ρ) and average atomic number (Z). The surface layer most likely has different Z and ρ than the bulk glass so the estimated range of penetration given is approximate.

FIGURE 1. Analyses of Corrosion Layers



90°C/14.7 psi



90°C/1500 psi

FIGURE 2. Surface Layers of 131/TDS Waste Glass

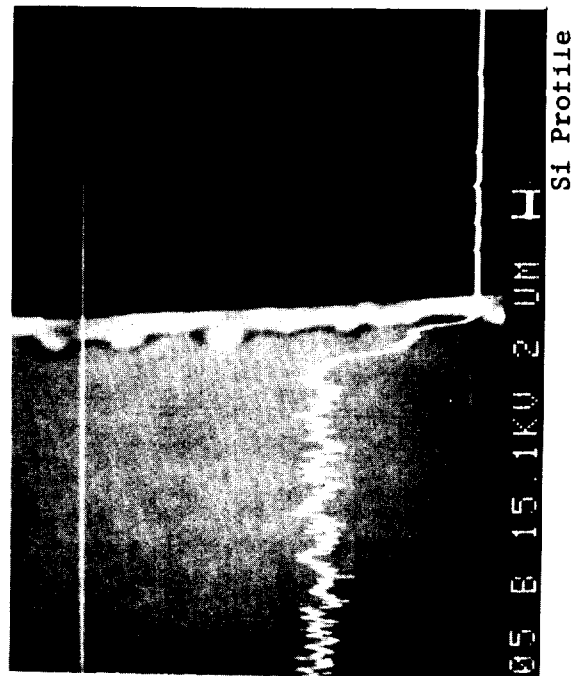
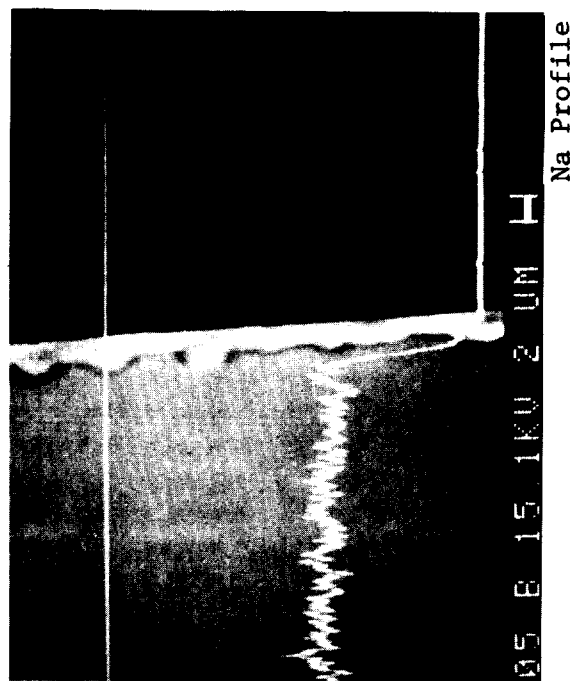
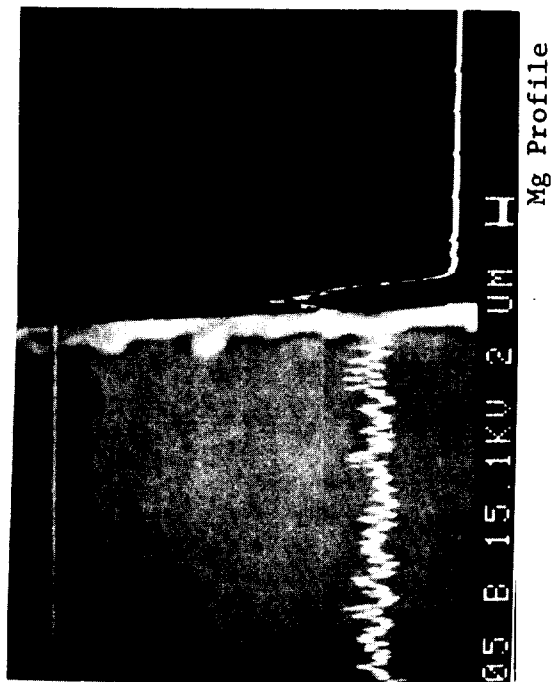
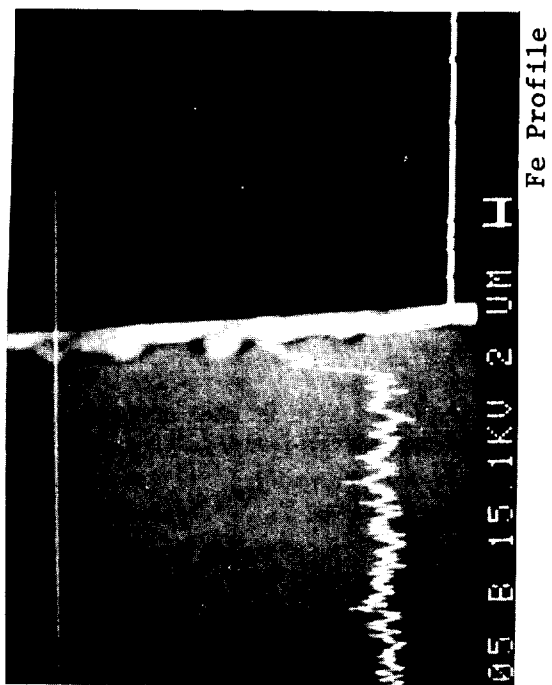


FIGURE 3. Cross Section of 131/TDS Waste Glass at 90°C and 1500 psi

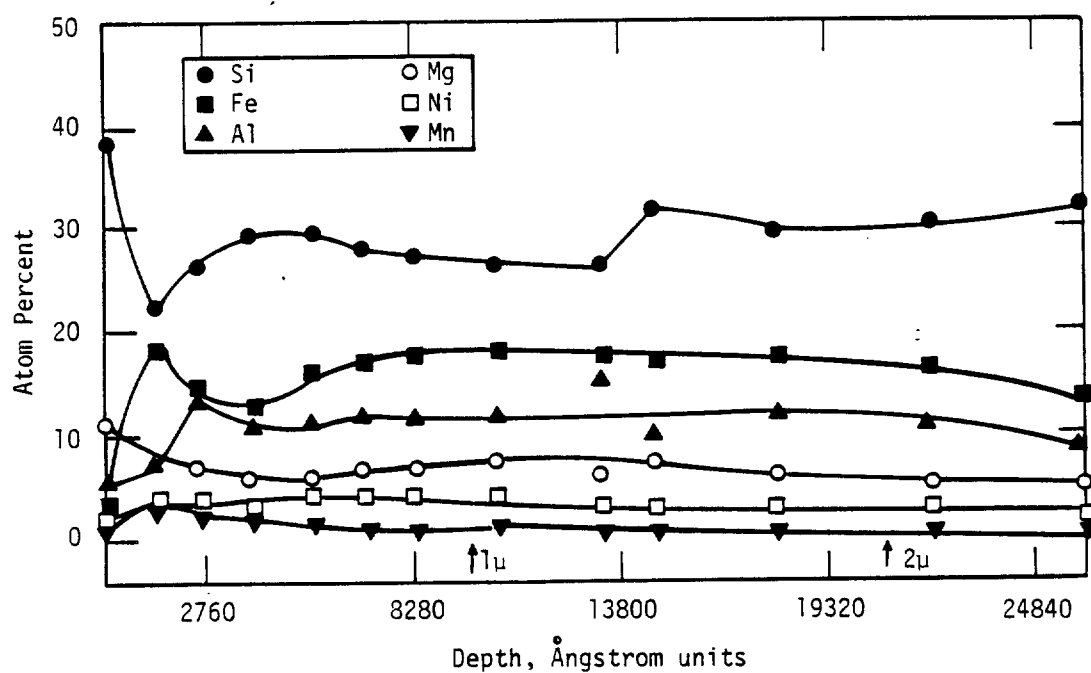


FIGURE 4. Depth Profile of Surface of TDS/131 Waste Glass
After Leaching at 90°C, 1500 psi as Measured by Auger Analyses

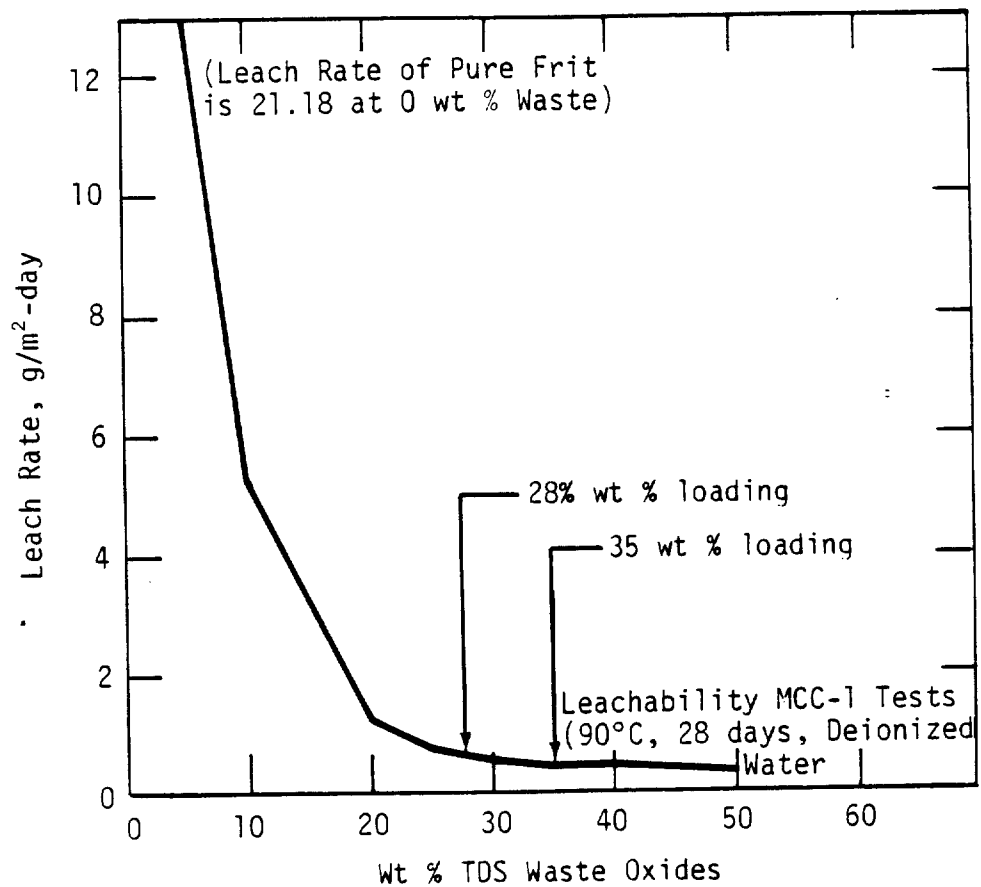


FIGURE 5. Leachability as a Function of Waste Loading

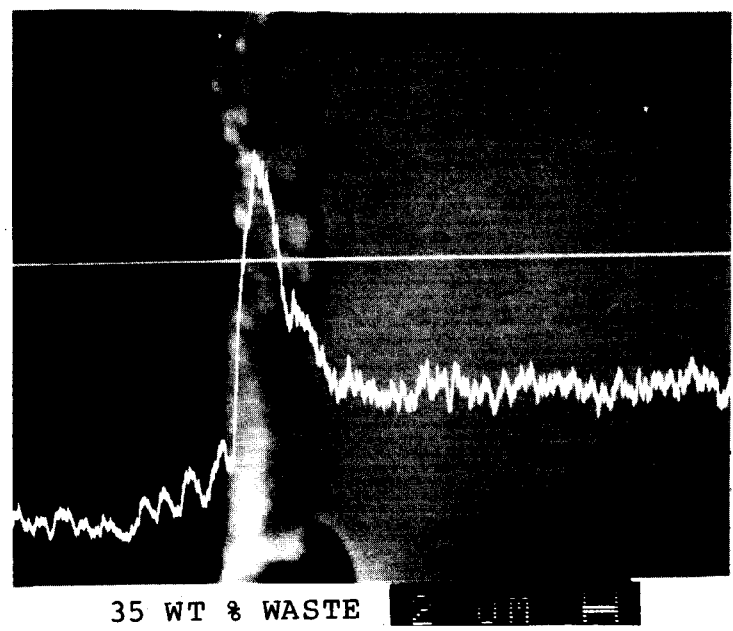
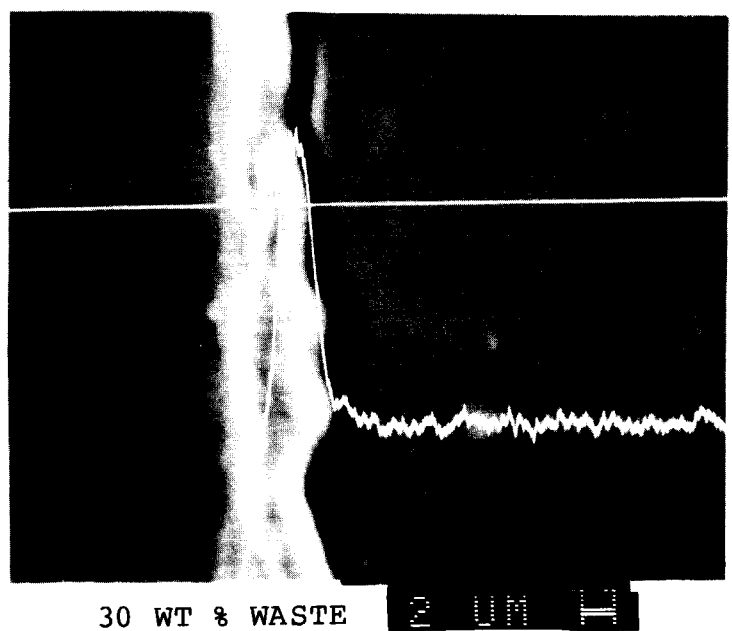
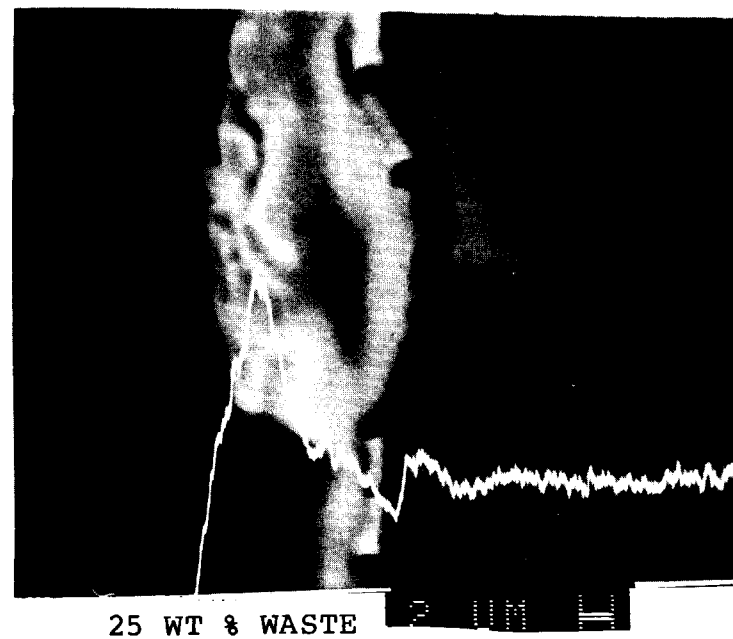
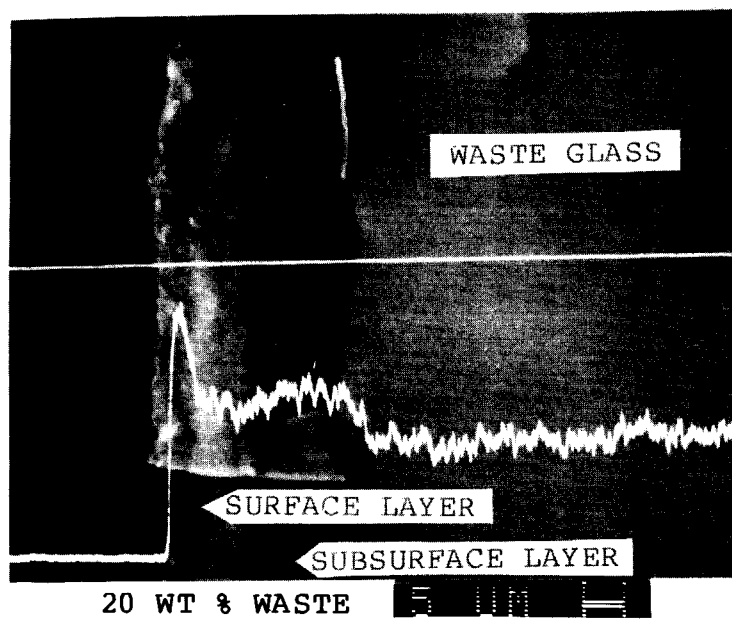
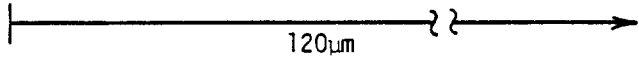

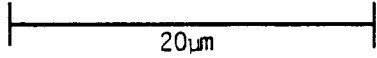
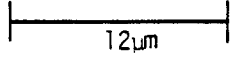
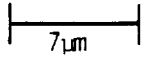
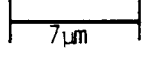
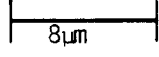
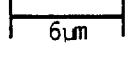


FIGURE 6. Surface Layer Characteristics as a Function of Waste Loading: Fe Profiles

% TDS Waste Oxides*	Surface Layer Thickness	Leachability, g/m ² -d
0**		21.18
10		5.22
20		1.19
25		0.73
30		0.51
35		0.41
40***		0.47
50		0.35

*Mixed with Frit 131.

**Surface layer of pure frit different than that of waste glasses.

***Special high temperature annealing treatment performed on this sample.

FIGURE 7. Schematic Representation of Average Surface-Layer Thickness and Corresponding Leachability as a function of Waste Loading

Si Represents all network formers in glass
 Na Represents all alkali elements in glass
 Fe Represents all heavy metal waste components

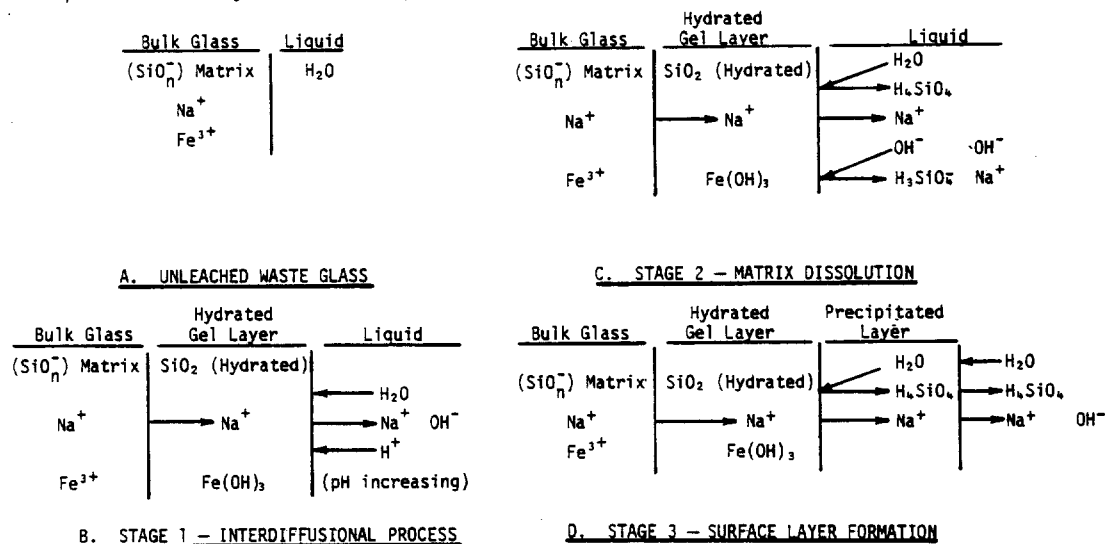


FIGURE 8. Schematic Representation of Corrosion of SRP Waste Glass

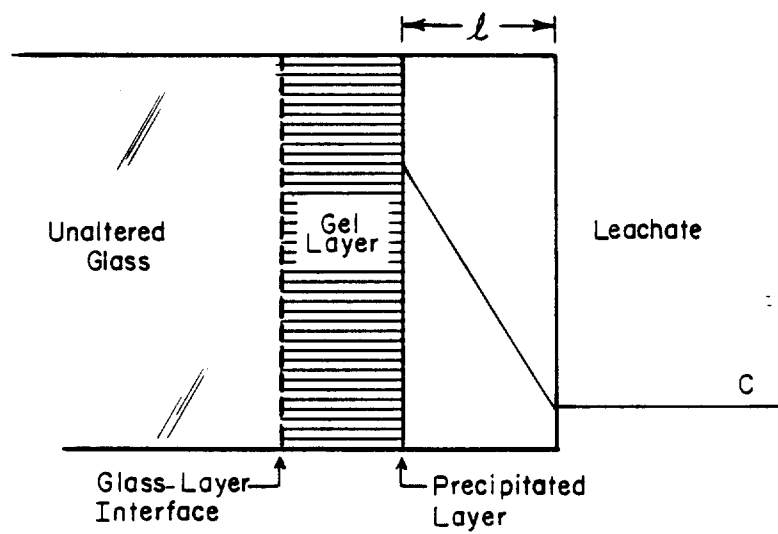


FIGURE 9. Model for Mathematical Treatment of Leaching of SRP Waste Glass Forms

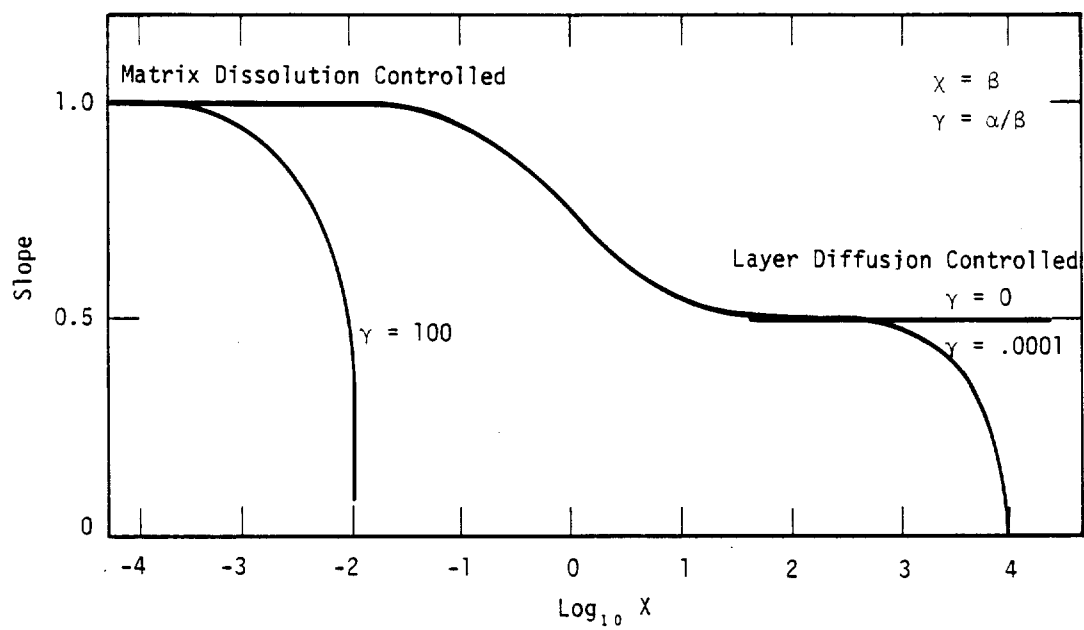


FIGURE 10. Slope of Log L Vs Log t as Function of x for Several Values of γ